REGULAR ARTICLE

A simple method of identifying π orbitals for non-planar systems and a protocol of studying π electronic structure

Tian Lu[1] · Qinxue Chen[1]

Abstract

The characteristic of π electrons has a crucial role in determining various properties of chemical systems, such as reactivity, aromaticity and spectroscopy. There are a large number of methods could be used for investigating π electronic structure, for example, the well-known electron localization function and multicenter bond order. For completely planar systems, the π molecular orbitals can be unambiguously identified and thus studying their π electronic structure is easy. However, for non-planar systems, identification of π orbitals and then analysis of π electrons are often not trivial. In this work, based on localized molecular orbitals (LMOs), we propose a conceptually simple and easy way to automatically identify π orbitals for any kind of systems, which makes subsequent analyses of π electrons straightforward. In addition, we show that the identified π LMOs can also be used to reliably estimate π component of molecular orbitals or other kinds of orbitals. The method proposed in this work has been implemented into our wavefunction analysis code Multiwfn as a key ingredient of standard analysis protocol for π electrons. Application examples given in this article illustrated that this protocol makes analysis of π electronic structure for a wide variety of chemical systems unprecedentedly convenient and reliable.

Keywords Orbital localization · Electron structure · Electron localization function · Multiwfn · Localized orbital locator · Electron density · π electron · Bond order

1 Introduction

For wide variety of organic systems and some inorganic species, π electrons have crucial role in determining their chemical and physical properties. For example, the nature of aromaticity and accompanied unique features of organic molecules stem from large range delocalization of π electrons; [1–3] the $n \rightarrow \pi^*$ and $\pi \rightarrow \pi^*$ types of electron transitions bring color for organic dyes; [4] the π–π stacking interaction essentially results from electron correlation effect between π electrons of closely packed aromatic rings; [5] the Diels–Alder reaction starts from interaction of π orbitals of reactants; [6] the delocalized π electrons over a ring

can generate strong induced current when external magnetic field is applied [7–9]. Obviously, due to the great importance of π electron, its analysis is indispensable in practical study of molecular electronic structure.

In the electronic wavefunction analysis framework, there have been a large number of methods that can be used to characterize π electrons, and several popular ones are briefly mentioned here. Note that in the present context, the σ orbitals refer to all orbitals except for the π ones.

- *Electron density and population* The electron density is a simple real-space function of representing distribution of electrons. The density of π electrons can be calculated as follows

$$\rho^\pi(\boldsymbol{r}) = \sum_{i \in \pi} \eta_i \left| \varphi_i(\boldsymbol{r}) \right|^2$$

where η is orbital occupation number, φ denotes orbital wavefunction, the index only loops over π orbitals.

The atomic π population is able to quantify the amount of π electrons carried by different atoms. It can be calculated in

✉ Tian Lu
  sobereva@sina.com
  http://www.keinsci.com

1 Beijing Kein Research Center for Natural Sciences, Beijing 100022, People's Republic of China

different ways, for example, using atomic space integration formalism:

$$p_A^\pi = \int_{\Omega_A} \rho^\pi(\mathbf{r}) \mathrm{d}\mathbf{r}$$

where A denotes an atom, the Ω signifies atomic space, which can be defined in various ways, such as Hirshfeld partition [10–12], Becke partition [13], AIM partition [14, 15] and so on. The π population can also be calculated in Hilbert space based on density matrix constructed from π orbitals by means of Mulliken population analysis or other schemes [12, 16].

- *Electron localization function (ELF) and its variants* The ELF is a very popular function for highlighting regions with high degree of electron localization [17–20]. It can also be used to vividly reveal electron delocalization paths [21, 22]. The ELF can be expressed as

$$ELF(\mathbf{r}) = \frac{1}{1 + [D(\mathbf{r})/D_0(\mathbf{r})]^2}$$

where $D(\mathbf{r})$ reveals the excess kinetic energy density caused by Pauli repulsion, the $D_0(\mathbf{r})$ can be interpreted as Thomas–Fermi kinetic energy density [23], both of them can be directly evaluated based on wavefunction and occupation number of orbitals. The ELF-π was proposed specifically for understanding localization and delocalization character of π electrons; it has been widely employed in studying aromaticity [24, 25]. The only difference between the ELF and ELF-π is that the latter only takes π orbitals into account.

There are several functions closely related to ELF and show similar distribution character, but with different definitions and underlying ideas. These functions include strong covalent interaction (SCI) [26], phase-space-defined Fisher information density (PS-FID) [27], localized orbital locator (LOL) [28, 29], region of slow electrons (RoSE) [30] and so on. Among which, the LOL has already been popular, it often shows a more clear picture than ELF. In addition, its variant, LOL-π, has been successfully used to investigate delocalization channel of π electrons [7].

- *Multicenter bond order (MCBO) and Mayer bond order* The MCBO is a method frequently employed in the literature to study the strength of multicenter electron conjugation and aromaticity [31–34]. The general expression of normalized MCBO is shown as follows

$$I_{ABCDEF\ldots K} = \left| \sum_{a \in A} \sum_{b \in B} \sum_{c \in C} \cdots \sum_{k \in K} (\mathbf{PS})_{ab}(\mathbf{PS})_{bc}(\mathbf{PS})_{cd} \ldots (\mathbf{PS})_{ka} \right|^{1/n}$$

where $\mathbf{P}$ and $\mathbf{S}$ correspond to density matrix and overlap matrix, respectively. The A, B, C… are indices of atoms, while a, b, c… denote indices of basis functions centered at respective atoms. n is the number of atoms constituting the ring. The normalization factor $1/n$ was suggested in Ref. [35] to make magnitude of MCBO values for rings with different number of members comparable.

The element of density matrix can be constructed from orbital expansion coefficients

$$P_{\mu\nu} = \eta_i \sum_i C_{\mu i} C_{\nu i}$$

where C corresponds to coefficient matrix, subscripts μ and ν denote indices of basis functions. The density matrix of π electrons ($\mathbf{P}\pi$) corresponds to the special case when orbital index only loops over π orbitals. If $\mathbf{P}\pi$ is used to estimate MCBO, then the result, MCBO-π, could be seen as a direct measure of π conjugation.

Formally, the Mayer bond order [36] may be viewed as a limiting case of MCBO when the number of involved centers is just two. It was shown that the value of Mayer bond order essentially reflects the average number of electron pairs shared among the two selected atoms [37], and thus it is expected that the Mayer bond order calculated based on $\mathbf{P}\pi$ can be used to quantify the average number of shared π electron pairs.

It is worthy to note that unlike electron density, the ELF, LOL, MCBO and Mayer bond order are not additive, namely their values cannot be exactly decomposed as sum of contributions from individual orbitals, but this point does not affect their practical usefulness in studying π electronic structure. Only for completely planar systems, it can be shown that separation of MCBO and Mayer bond order as sum of σ and π contributions is rigorous.

A key difficulty of applying above valuable analyses in investigating π electrons of practical systems is how to quickly and unambiguously identify occupied π orbitals. Usually, the aforementioned functions or quantities are calculated based on molecular orbitals (MOs). For planar systems, the π MOs can be identified according to the standard definition, namely there should be a nodal plane along the geometric plane of the system. Unfortunately, for large systems, manually identifying all occupied π MOs by visually inspecting their isosurfaces is often a quite laborious task. For non-planar systems, the situation is much more involved. Due to unavoidable mixing between σ and π orbitals, it is difficult and sometimes impossible to judge if a MO could be regarded as π type.

The main aim of present work is to propose a simple but robust way of automatically identifying π orbitals and thus making aforementioned π electron analysis methods applicable to systems with arbitrary geometric characters. The new algorithm described in this work has been implemented in our wavefunction analysis code Multiwfn [38], which is freely available at http://sobereva.com/multiwfn.

Since all analysis methods mentioned above have already been well supported by Multiwfn, implementation of the new automatic π orbital identification technique into Multiwfn makes all of the analyses for wide variety of practical systems unprecedentedly easy.

The rest part of this article is organized as follows: In Sect. 2, we introduce the idea and implementation details of our π orbital identification method; in Sect. 3, we outline the framework of π electron analysis protocol in Multiwfn code. In Sect. 4, some illustrative applications are given to demonstrate the reliability, universality and practical value of the π orbital identification algorithm and the π electron analysis protocol. In the final section, we summarize this article and make a few remarks.

2 Algorithm of automatically identifying π orbitals and evaluating orbital π component

For a completely planar or nearly planar system, identifying its π MOs is relatively easy. Assume that all atoms are in XY plane, it is naturally expected that an ideal π MO should purely composed of p_z atomic orbitals. In order to tolerate the situation with slight out-plane structure distortion, we define following rules to detect π MOs. All MOs that simultaneously satisfy these two conditions should be considered to be π type.

(1) Absolute value of coefficient of any S, PX, PY type of Gaussian type function (GTF) is less than 0.1
(2) Orbital composition contributed by all PZ type of GTFs is higher than 80%. For simplicity, SCPA method [39, 40] is used to estimate the composition.

For evidently non-planar or highly distorted systems, defining a general rule of identifying π MOs is never so straightforward, and it is frequently observed that numerous MOs exhibit severe σ–π hybrid character. In this case, the best and may be the only way to represent the π electrons in terms of orbital picture should be performing orbital localization to yield localized molecular orbitals (LMOs) first, and then identifying π type of LMOs according to certain criterion defined based on LMO feature. Our suggested process of judging if an orbital could be attributed as π type is given below

(1) Calculating orbital composition to determine the atoms having the largest and second largest contributions, which will be referred to as A and B, respectively.
(2) If contribution of A to the orbital is larger than a threshold (85%), then the orbital should be viewed as single-center and thus be ignored.
(3) Calculating orbital density, namely $|\varphi(\mathbf{r})|^2$, at two probe points with coordinate of $0.7\mathbf{R}_A + 0.3\mathbf{R}_B$ and $0.3\mathbf{R}_A + 0.7\mathbf{R}_B$, where $\mathbf{R}_A$ and $\mathbf{R}_B$ are coordinates of atoms A and B, respectively, see Fig. 1 for graphical illustration.
(4) If orbital density at the two probe points is simultaneously lower than a threshold (0.01), then the orbital is finally identified as π type.

The idea of defining the above rules and the reason for introducing the density threshold are easy to understand: If an ideal π orbital forms between two atoms, since this kind of orbital has a nodal plane along the bond, the orbital density at the two probe points placed along the linking line between the two atoms should be exactly zero. However, when the two atoms are not in a planar local region (for example, the C–C bond in fullerene), σ and π orbitals will not be strictly separable due to unavoidable σ–π mixing, and correspondingly, the orbital density along the linking line is not fully vanished; hence, a threshold must be set to tolerate this circumstance.

Once indices of π MOs or π LMOs have been determined according to the procedure described above, before conducting analyses of π electronic structure, the only additional thing should do is setting occupation number of all other orbitals to zero and accordingly reconstruct density matrix. It is worth to emphasize that analyzing π electrons based on

Fig. 1 Illustration of a π LMO of 1,3-butadiene. The two cyan spheres display the probe points of orbital density between the two carbon atoms at a boundary C–C bond
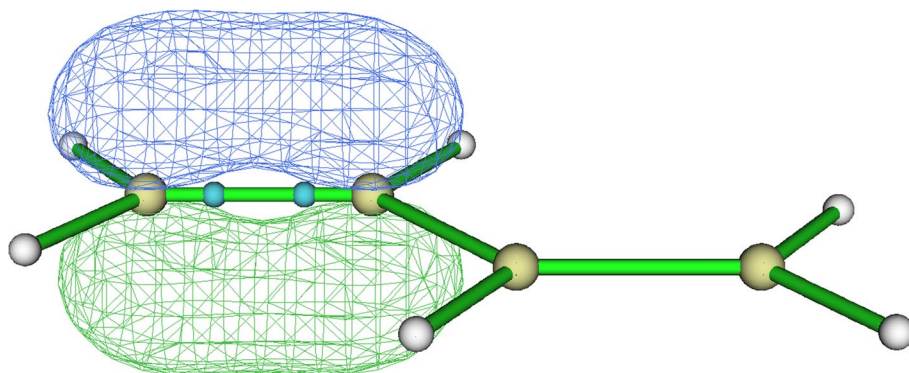
LMOs is essentially as reasonable as analyzing them based on MOs. All the analysis methods mentioned in Sect. 1 only involve density matrix or real-space functions with definitive physical meaning, and therefore the analysis results are invariant to unitary transformation between π MOs and π LMOs [41], in other words, the results are identical irrespective of representing π electrons in terms of MOs or LMOs.

Totally three empirical parameters are involved in our π orbital identification method for non-planar case, namely the single-center contribution threshold, the orbital density threshold and the position of probe points at the interatomic linking line. According to our experiences and tests, the current setting has the best compatibility with wide variety of systems and orbitals.

Our method of identifying π LMOs is compatible with Pipek–Mezey [42], Edmiston–Ruedenberg [43] and natural localized molecular orbital (NLMO) [44] orbital localization methods because their resulting LMOs show separated character of σ and π for multiple-bonds [45]. It is important to note that Foster-Boys localization method [46] should not be used in conjunction with our identification method, since Foster-Boys localization represents a multiple-bond as multiple "banana bonds," which shows strong hybrid σ and π characters.

There is no unique method of computing orbital composition [39]. Hirshfeld, Becke, SCPA and Mulliken orbital composition analysis methods are currently supported by Multiwfn for the automatic π orbital identification purpose. Despite that the Hirshfeld and Becke methods are more robust for evaluating atom contributions to orbitals [39], it is found that the SCPA method, which has negligible computational cost, works equally well in identifying π orbitals, and therefore it is more recommended to use. However, it is

well known that diffuse functions often make SCPA analysis meaningless [39], and therefore Hirshfeld or Becke method should be adopted instead when the basis set contains diffuse functions.

A useful byproduct of the π LMO identification algorithm is the quantitative estimation of orbital π character. The π component of a given orbital could be obtained via orthogonal projection technique:

$$\Theta_i^\pi = 100\% \times \sum_j^{\pi\text{LMO}} c_{j,i}^2$$

the $c_{j,i}$ is projection coefficient from the orbital i to π LMO j:

$$c_{j,i} = \langle j \mid i \rangle = \sum_\mu \sum_\nu C_{\mu,i} C_{\nu,j} \langle \chi_\mu \mid \chi_\nu \rangle$$

where χ is symbol of basis function. The orbital π component is useful in many theoretical chemistry studies. For example, percentage π–π* transition character in an electron excitation process can be studied based on the π component of the mainly involved MOs.

3 Protocol of π electron analysis in Multiwfn code

Based on the new identification method for π orbitals, we propose a standard protocol for realizing π electron analysis, as shown in Fig. 2. All ingredients have been supported by our Multiwfn code. The basic process of using Multiwfn to carry out π electron analysis as well as some details of implementation is described below.

Fig. 2 Flowchart of standard π electron analysis protocol
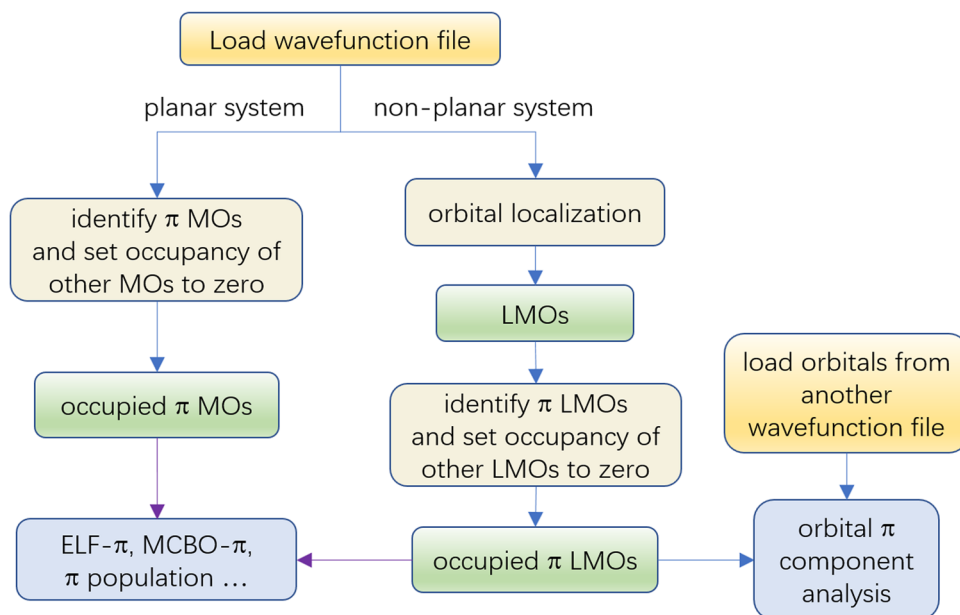
(1) *Loading wavefunction file* If the system is non-planar and thus orbital localization is needed, the inputted wavefunction file must contain basis set definition and coefficient matrix with respect to basis functions.fch/.fchk file, Molden input file (.molden) and some other files could be employed as input file in this situation. If the system is planar and thus MOs can be directly subjected to π orbital identification, then.wfn and.wfx formats can also be used.

(2) *Orbital localization* For non-planar or distorted systems, the loaded MOs should be transformed to LMOs by the orbital localization module of Multiwfn. Commonly only localizing occupied MOs is adequate. Without special reason, the Pipek–Mezey localization method should be adopted, not only because it has ability to separate σ and π characters, but also it is the most inexpensive orbital localization method. Of course, orbital localization could be skipped if the system is planar.

(3) *Identifying π orbitals* In Multiwfn, the module for identifying π orbitals is quite general and flexible, the type of supported orbital is not limited to MO or LMO, and others such as natural orbital (NO) [45], natural transition orbital (NTO) [47] and natural bond orbital (NBO) [48] are also acceptable. Users will be asked to choose the character of the present orbitals, and the two different algorithms described in last section are, respectively, used to identify the orbitals showing delocalized character (*e.g.*, MO, NO, NTO) and those showing localized character (*e.g.*, LMO, NBO). The interface of this module provides many options so that users can customize relevant parameters, set constraint on π orbital searching, choose method for computing orbital composition and so on.

(4) *Modifying orbital occupancy status* In order to study π electrons in the subsequent analyses, contribution due to σ orbitals should be excluded. In Multiwfn, real-space functions such as electron density and ELF are evaluated based on orbital wavefunctions and their occupation numbers, while most other analyses such as MCBO and Mulliken population analysis are calculated based on density matrix. In this stage, Multiwfn asks users to set occupation number of the identified π orbitals or that of other orbitals. To analyze π electrons, users should choose to clean the occupation number of σ orbitals. After that, Multiwfn correspondingly updates density matrix.

(5) *π electron analysis* Since both orbital occupation numbers and density matrix currently only reflect π electrons, all wavefunction analyses performed by the users directly correspond to the analyses of π electrons.

In addition, if one would like to calculate π component of specific set of orbitals, in the π orbital identification interface, another wavefunction file should be provided, and the identified π LMOs will be automatically used to evaluate percentage π character for selected orbitals in the second wavefunction file.

4 Illustrative applications

In the next subsections, we take a few systems to illustrate the reliability, applicability, flexibility and practical value of the π electron analysis protocol described above. All quantum chemistry calculations were conducted by Gaussian 16 A.03 program [49]; Multiwfn 3.7(dev) code [38] was used for wavefunction analysis. Default parameters for identification of π orbitals were used for all studies, and SCPA and Pipek–Mezey methods were chosen to evaluate orbital composition and localize occupied MOs, respectively. Unless otherwise specified, generation of wavefunction and geometry optimization were conducted at the B3LYP/6-31G* level [50, 51]. Increasing the quality of basis set or altering exchange–correlation functional do not detectably affect the analysis results. Despite Multiwfn has a built-in interface for directly viewing isosurface of real-space functions, all isosurface graphs were rendered by VMD program [52] to gain better visual effect.

4.1 π electron distribution on nanotube fragment

The first example is a saturated nanotube fragment of (6,6) chirality, and there are totally 84 carbon and 24 hydrogen atoms. All occupied MOs recorded in.fch file yielded by Gaussian program were subjected to orbital localization. On an Intel four-core CPU (i7-2630QM) this process only takes less than 1 min. The time spent for identification of π LMOs is negligible (no more than 1 s). Totally 42 occupied π LMOs were finally identified under default setting. This observation is fully in line with chemical intuition, namely each carbon atom contributes a π electron, and thus the 84 π electrons due to the 84 carbons correspond to 42 closed-shell orbitals.

After setting occupation number of all σ LMOs to zero to eliminate their contributions to subsequent analyses, electron density grid data were calculated to characterize distribution of π electrons. The isosurface map of $\rho\pi = 0.04$ a.u. is shown as Fig. 3a. From the occurrence region and shape of the isosurface, it is clear that the actual distribution of the π electrons has been faithfully revealed, and well demonstrating that the protocol of identifying π orbitals and analyzing π electrons proposed in this work is reasonable. This figure also implies that the density of π electrons is higher on the inner side of the carbon nanotube than on the outer side,

Fig. 3 π electronic structure of a fragment of saturated nanotube **a** Isosurface map of π electron density with isovalue of 0.04 a.u. **b** Colored map showing π population on carbons calculated by Mulliken analysis
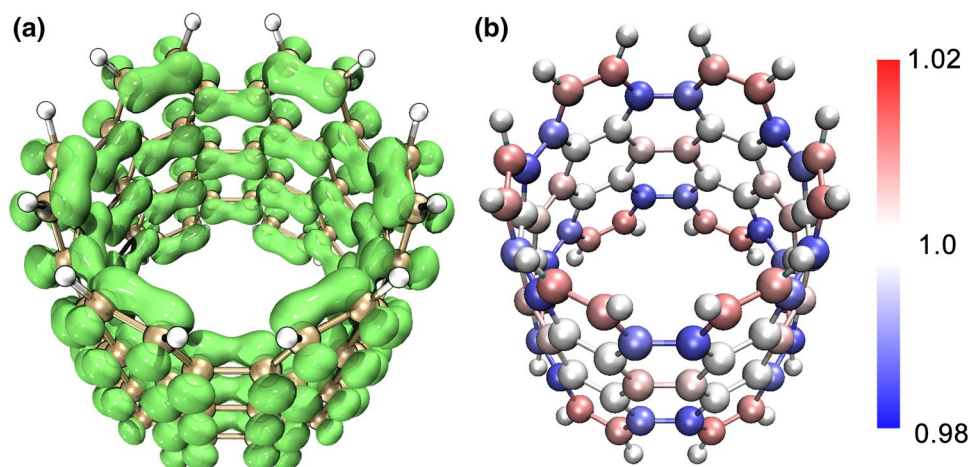
because on the outer side, the isosurface over each carbon is fully isolated, while in the inner side some neighboring carbons show merged isosurface because of relatively higher density in their π bonding regions.

It is not easy to compare difference in total amount of π electrons between various atoms based on the isosurface map, because the number of π electrons carried by different atoms has similar magnitude. In contrast, π population is quite appropriate for distinguishing this difference, even if the difference is marginal. After setting occupation number of all σ LMOs to zero, Mulliken population analysis was performed and the atoms are colored according to the resulting atomic π populations, see Fig. 3b. In this map, the colors vividly exhibit the quantitative difference in π electron distribution at different sites.

4.2 LOL-π and π component of MOs of 6-helicene

The 6-helicene consists of six connected six-membered carbon rings and has highly curled structure. For such a complicated system, it is quite difficult to manually identify all appropriate orbitals for revealing its π electronic structure, while our protocol makes π electron analysis of this molecule quite easy and convenient. Figure 4 shows isosurface map of the LOL-π constructed based on the automatically identified π LMOs, and isovalue of 0.55 is adapted because in this case the map is able to distinguish delocalization extent of the π electrons on different rings. From the figure, it can be seen that the LOL-π map successfully revealed delocalization channel of the π electrons. From the figure, it can also be inferred that the two rings at the two ends have stronger six-center conjugation, because under the current isovalue setting, the LOL-π isosurfaces over the two terminal six-membered rings are fully connected, while the isosurfaces over the other rings are partially disconnected.

We also calculated MCBO based on the density matrix solely contributed by the π LMOs and labeled the result on
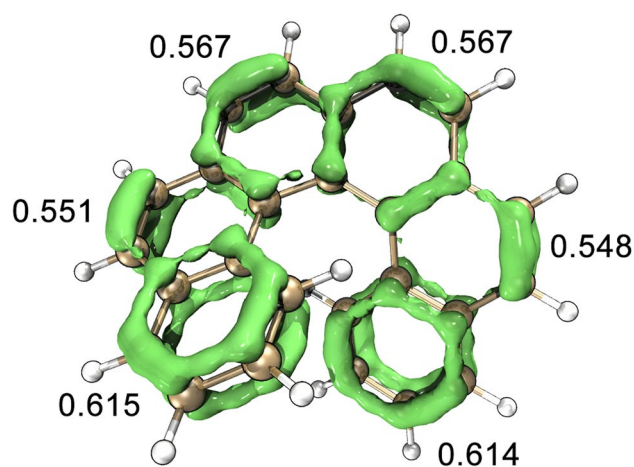

Fig. 4 LOL-π isosurface of 6-helicene with isovalue of 0.55. The normalized six-center bond order of the six rings is also labeled

Fig. 4. From the difference in MCBO-π values, one can easily conclude that the π electrons at the two terminal rings formed more evident six-center delocalization than the other rings; this conclusion is in good agreement with that observed from the LOL-π isosurface.

As mentioned earlier, based on the identified π LMOs, the quantitative π component of MOs could be evaluated. The percentage π character of four arbitrarily selected MOs of the 6-helicene is shown in Fig. 5. In order to verify whether or not the calculated values are really reasonable, the isosurface maps of the MOs are also shown together for comparison purpose. From Fig. 5, it can be seen that the MO65 shows largest σ–π mixing among the four MOs, and its π component is only 58.2%. This point is also understandable from the orbital isosurface map; as highlighted by the red circles, its isosurface exhibits apparent σ character at the two ends of the system. Both the isosurface map of MO78 and the quantitative value (78.4%) show that MO78 possesses relatively higher π character

Fig. 5 Isosurface map of four selected molecular orbitals of 6-helicene with isovalue of 0.4. Green and blue colors correspond to positive and negative phases of orbital wavefunction, respectively. The percentage π components of these orbitals are labelled, and the red dash circles highlight the regions showing evident σ character
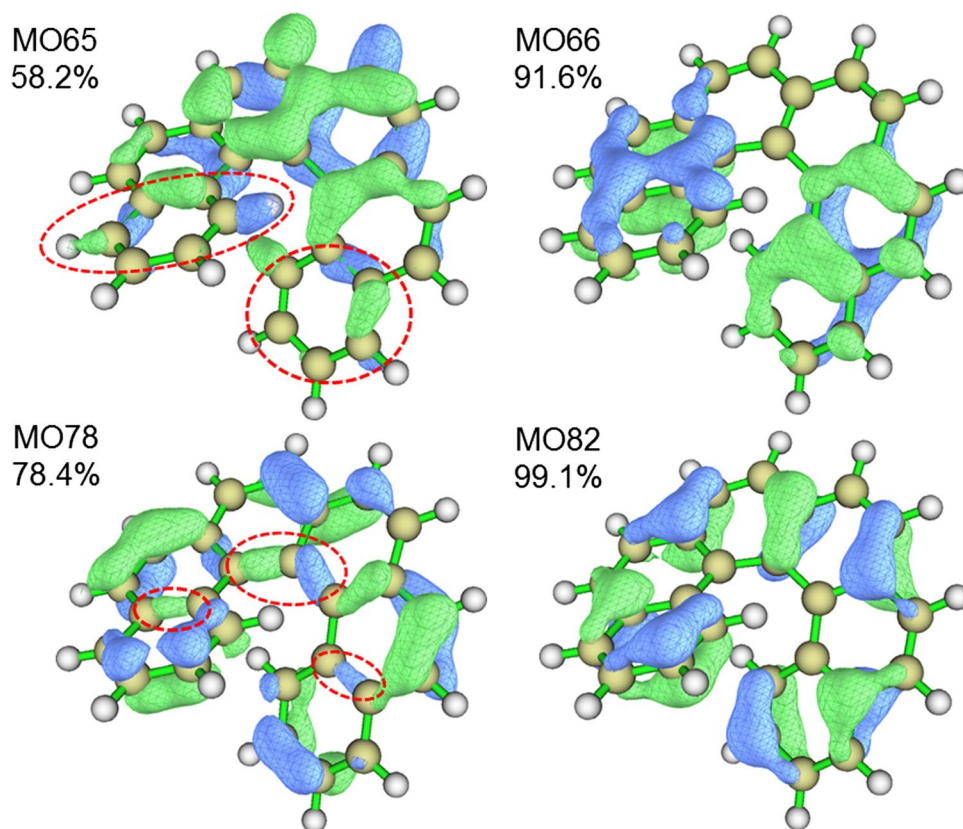

than MO65. The MO82 has π character of 99.1%, indeed, in the regions where its isosurface appears the orbital always has a clear nodal plane along the ring. Obviously, the MO82 completely conforms to the common definition of π orbital and can be regarded as a perfect π MO. This example fully demonstrated that our proposed method for estimating orbital π component is reliable, thus when one is looking for the MOs exhibiting significant π feature, it is no longer necessary to tediously inspect orbital isosurfaces one by one.

4.3 π Mayer bond order and topology analysis of ELF-π of corannulene

Corannulene is a kind of bowl like polycyclic aromatic hydrocarbon, and its structure, aromaticity and reactivity have been thoroughly investigated recently [53]. In this example, the ELF-π analysis and π Mayer bond order were carried out based on our π electron analysis protocol, and the isosurface map of ELF-π and bond order data are shown in Fig. 6.

Fig. 6 Isosurface map of ELF-$\pi = 0.7$ of corannulene. **a** and **b** correspond to convex and concave sides of the molecule, respectively. Blue spheres highlight positions of $(3, -1)$ type of ELF-π critical points, while blue texts indicate exact ELF-π value at these points. The red texts show value of π Mayer bond order of the four symmetry unique C–C bonds
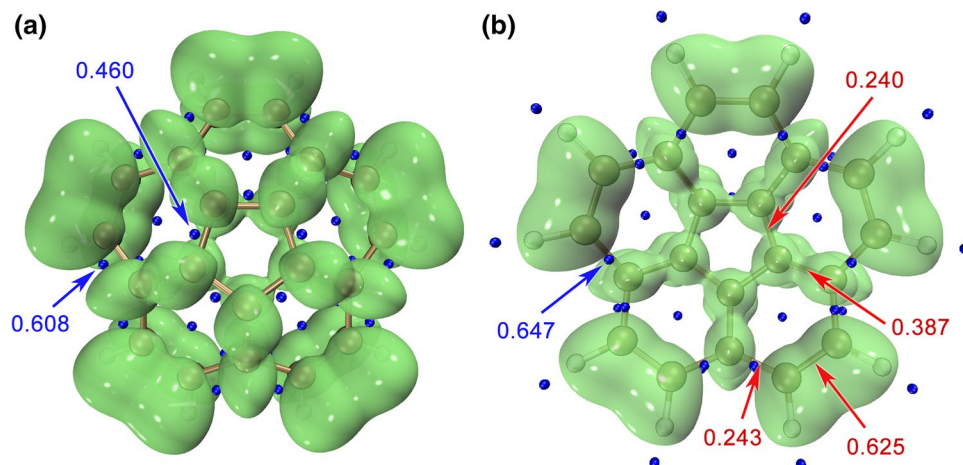
From Fig. 6, it can be seen that like the LOL-π utilized in previous example, the ELF-π isosurface also well exhibits π electron delocalization of present system. When investigating molecular aromaticity, the ELF-π is often studied in terms of bifurcation point [25], which is equivalent to the $(3, -1)$ type of critical point defined in the topology analysis framework [14]. The bifurcation point of ELF-π is the position where an ELF-π domain just separates as two adjacent domains as the isovalue increases. It is argued that the larger the ELF-π value at the bifurcation point, the higher the degree of electron delocalization between the two separated ELF-π domains. The blue spheres in Fig. 6 display that on each six-membered ring, there are three and two bifurcation points at the convex and concave sides, respectively. On the convex side, the ELF-π values at the bifurcation points (0.608 and 0.460) suggest that π delocalization along the outer edge of the corannulene is more favorable than along the edge of the internal five-membered ring.

To further quantify π electron delocalization between bonded atoms, Mayer bond orders were evaluated based on density matrix deriving from occupied π LMOs, and the results are shown in Fig. 6b using red texts. The value of the π Mayer bond orders is consistent with the information conveyed by the ELF-π map. For example, there is no ELF-π bifurcation point on the outermost five C–C bonds of the corannulene, and meantime these bonds are fully enclosed by the ELF-$\pi = 0.7$ isosurfaces; this observation implies strong π interaction; correspondingly, these bonds have large π Mayer bond order (0.625), which are conspicuously higher than other bonds.

4.4 Ru(bpy)$_3^{2+}$ complex

Next, a more challenging system, Ru(bpy)$_3^{2+}$ transition metal complex, is taken as a test case to examine if our π orbital identification algorithm can be applied to broader types of molecules other than purely organic ones. The geometry optimization was carried out using BP86 exchange–correlation functional [54, 55], 6-31G* [50] and SDD pseudopotential basis sets [56] were adopted for ligand atoms and Ru atom, respectively. The wavefunction to be analyzed was generated at the same level. The LOL-π was employed to examine if π electrons can be faithfully unveiled. According to the shape and distribution of the LOL-π isosurfaces in Fig. 7, it is obvious that our automatic π orbital identification method also works well for this system, since all regions where π electrons should exist are correctly outlined by the LOL-π isosurface, and meantime there is no isosurface occurs in undesired regions, such as those around C-H bonds and Ru atom.
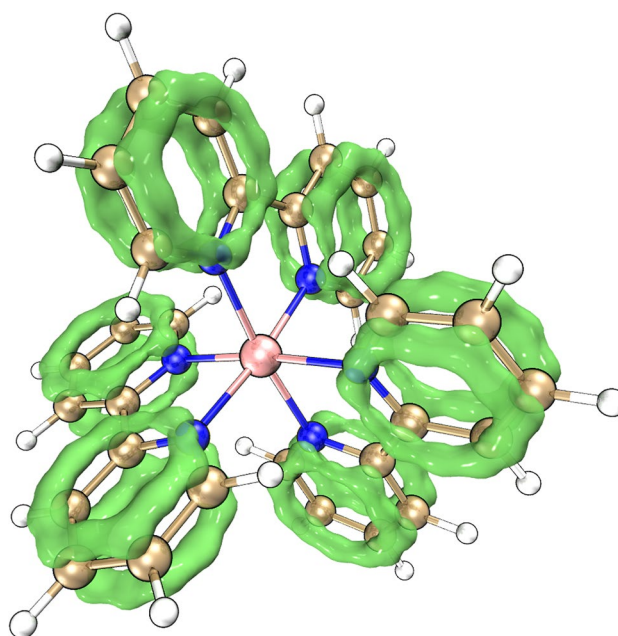

Fig. 7 Isosurface map of LOL-π of Ru(bpy)$_3^{2+}$ transition metal complex with isovalue of 0.5. Pink, blue, brown and white spheres correspond to Ru, N, C and H atoms, respectively

4.5 Stacked complexes

The system studied in this section is stacked circumcoronene and hydrogen-bonded guanine–cytosine dimer, and the geometry employed in this study is the theoretically predicted one provided in Ref. [57]. This system not only contains many heteroatoms but also consists of more than one molecule, and therefore it could be served as a good instance for testing universality and robustness of our π electron analysis protocol.

Figure 8 shows isosurface map of LOL-$\pi = 0.4$. As expected, wide range delocalization nature of the π electrons over the circumcoronene is very clearly represented. The isosurfaces also occur above and below the guanine plane, rendering the fact that the guanine also possesses largely delocalized π electrons. The close contact of LOL-π isosurfaces of the monomers in this figure vividly delineates the π–π stacking in this system, providing a complementary picture for the popular NCI analysis method [8, 38, 58], which is able to graphically reveal the occurrence region of weak interactions. From Fig. 8, it can also be found that there is no LOL-π isosurface on the amino group of guanine moiety; this is a desirable phenomenon since the lone pair of the amino group does not participate into the π conjugation.

The flexible π orbital identification module of Multiwfn allows users to set constraint by defining an atomic list, if any of the two atoms having largest orbital contribution does not belong to the atomic list, then this orbital will be impossible to be recognized as final π orbitals. In

Fig. 8 Isosurface map of LOL-π of stacked circumcoronene and hydrogen-bonded guanine–cytosine dimer. Isovalue of 0.4 is employed. The cytosine moiety was excluded during π LMO identification process
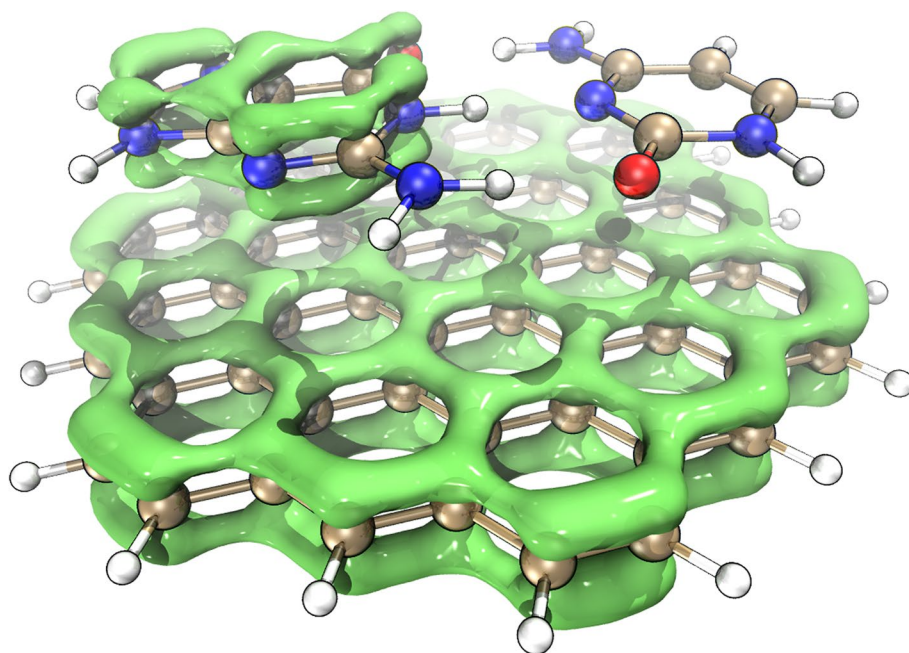

the process of identifying π LMOs for present system, a constraint was applied to request the program to ignore all LMOs located on the cytosine moiety. The fully vanished isosurface on the cytosine moiety in Fig. 8 proved the success of the customized constraint, demonstrating that the spatial range in which π electrons are investigated can be fully controlled.

4.6 [Pt(trpy)(C≡CPh)]$^+$ cationic complex: π orbitals involving d atomic orbitals

The final example is [Pt(trpy)(C≡CPh)]$^+$, whose ground state geometry is nearly planar, see Fig. 9. The ligands show strong global π conjugation character, and therefore it is expected that the d atomic orbitals of the central Pt atom may be somewhat involved in the π orbitals. In this section,

Fig. 9 Optimized geometry of [Pt(trpy)(C≡CPh)]$^+$ cationic complex and its three localized molecular orbitals, which are mainly contributed by d type of atomic orbitals of Pt atom and have partial delocalization character. Isovalue of 0.02 is used to render the orbital isosurfaces. The composition of Pt atom in the orbitals evaluated by Hirshfeld method is given in the parenthesis

LMO87 (85.7%)   LMO88 (85.9%)   LMO90 (88.9%)
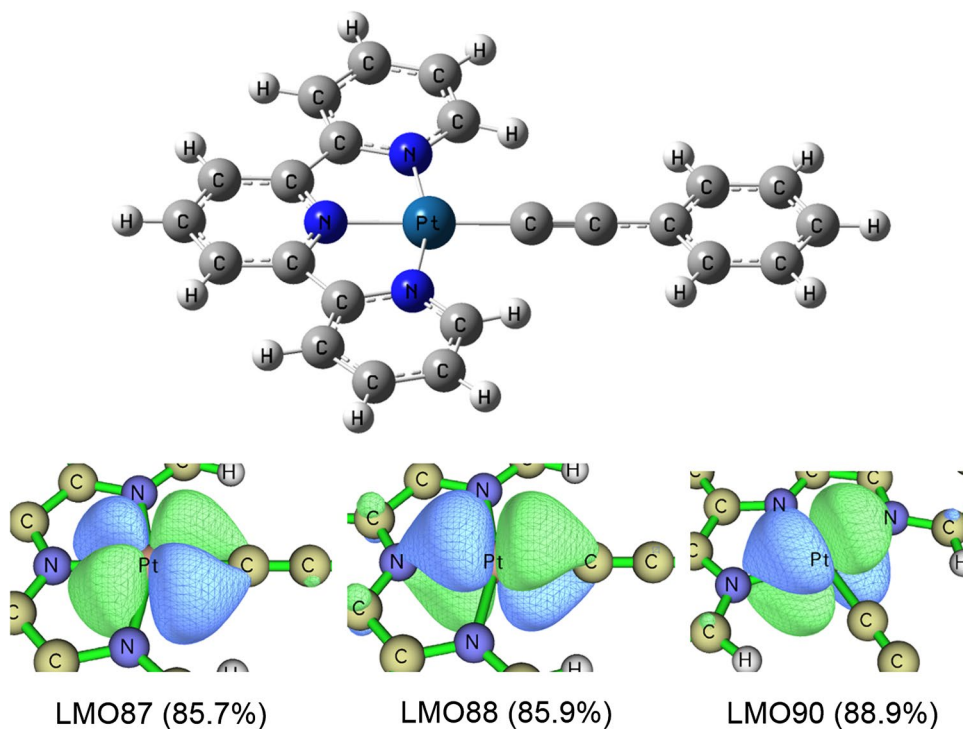
we check whether or not the participation of the *d* electrons in the π orbitals can be revealed by our new method.

From Fig. 9, it can be seen that in the [Pt(trpy)(C≡CPh)]$^+$ there are three LMOs mostly contributed by the *d* atomic orbitals of the Pt atom; however, they also partially delocalize to ligand atoms, as vividly shown by the shape of orbital isosurfaces and quantitatively exhibited by the orbital compositions. According to the nodal plane character, these LMOs may also be regarded as π orbitals. We found that when Hirshfeld method is used to compute orbital compositions and default thresholds for identifying π orbitals are employed, only π LMOs in ligands can be recognized, the resulting LOL-π isosurface map is given as Fig. 10a. However, if the condition for determining single-center orbitals is tightened, namely increasing the orbital composition threshold from the default 85% to 90%, then the three LMOs shown in Fig. 9 will also be identified as bonding π orbitals, making the weak π interaction between the ligand atoms and the three *d* atomic orbitals of the Pt atom detectable in the LOL-π map, as exhibited in Fig. 10c. This instance demonstrates that our π orbital identification method is also applicable when *d* atomic orbitals are involved as long as proper thresholds are employed.

5 Summary

There have been a large number of valuable analysis methods that may be used for characterizing π electrons, unfortunately in most cases analyzing π electronic structure is inconvenient and even impractical, especially for large or non-planar ones, because it is often quite difficult to quickly and properly select orbitals that specifically describe π electrons. Considering the fact that the localized molecular orbitals (LMOs) have a highly localized feature and identifying type of LMOs is usually much easier than that of MOs, we proposed an algorithm to automatically identify π LMOs; based on which, we designed a standard protocol of performing π electronic structure analysis and implemented it in our wavefunction analysis code Multiwfn. Several application instances fully demonstrated the robustness of the automatic π orbital identification method as well as the value of the analysis protocol. Our method and code make applying popular electronic structure analysis methods such as ELF, LOL, MCBO and Mayer bond order for π electrons of wide variety of chemical systems unprecedentedly convenient.

As a byproduct of the π LMOs identification process, we also proposed a scheme of quantitatively evaluating π character for arbitrary kind of orbitals. This quantity could be useful at many aspects in theoretical chemistry studies. For example, π component of natural transition orbitals [47] may be used for quantitatively estimating percentage π–π* and n–π characters in electronic transitions, while π component of MOs may be employed as a criterion for screening active orbitals involved in the complete active space self-consistent field (CASSCF) calculation [45].

Considering the length of the article, operation steps of the π electron analyses in Multiwfn are not explicitly given in the text; however, the users can easily and quickly learn how to use the code to perform these analyses by following the detailed tutorials in the program manual [59]. It is worth to mention that although the default parameters of identifying π orbitals work well for all of our test systems, it is still possible that in rare cases one or more π LMOs cannot be properly recognized, in that case the users are encouraged to slightly adjust the parameters by corresponding options until the result meets expectation.

Fig. 10 Isosurface map of LOL-π of [Pt(trpy)(C≡CPh)]$^+$ **a** Isovalue is set to 0.35, default thresholds for identifying π LMOs are employed. **b** Isovalue is also set to 0.35, but the orbital composition threshold for determining single-center orbitals is increased from the default 85% to 90%. **c** The same as (**b**), but isovalue is lowered to 0.18 to better reveal the π interaction between the ligand atoms and the Pt atom
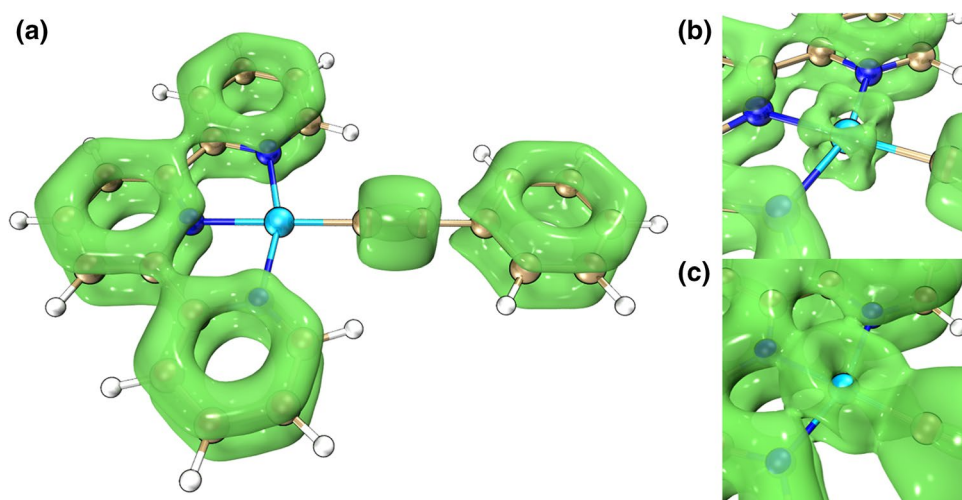
References

1. Yu D, Rong C, Lu T, Chattaraj PK, De Proft F, Liu S (2017) Aromaticity and antiaromaticity of substituted fulvene derivatives: perspectives from the information-theoretic approach in density functional reactivity theory. Phys Chem Chem Phys 19:18635

2. Yu D, Rong C, Lu T, Proft FD, Liu S (2018) Aromaticity study of benzene-fused fulvene derivatives using the information-theoretic approach in density functional reactivity theory. Acta Phys Chim Sin 34:639

3. Yu D, Stuyver T, Rong C, Alonso M, Lu T, De Proft F, Geerlings P, Liu S (2019) Global and local aromaticity of acenes from the information-theoretic approach in density functional reactivity theory. Phys Chem Chem Phys 21:18195

4. Klessinger M, Michl J (1994) Excited states and photochemistry of organic molecules. VCH Publishers Inc, New York

5. Grimme S (2008) Do special noncovalent π–π stacking interactions really exist? Angew Chem Int Ed 47:3430

6. Yang Y-F, Liang Y, Liu F, Houk KN (2016) Diels-Alder reactivities of benzene, pyridine, and di-, tri-, and tetrazines: the roles of geometrical distortions and orbital interactions. J Am Chem Soc 138:1660

7. Liu Z, Lu T, Hua S, Yu Y (2019) Aromaticity of Hückel and Möbius topologies involved in conformation conversion of macrocyclic [32]Octaphyrin(1.0.1.0.1.0.1.0): refined evidence from multiple visual criteria. J Phys Chem C 123:18593

8. Lu T, Manzetti S (2014) Wavefunction and reactivity study of benzo[a]pyrene diol epoxide and its enantiomeric forms. Struct Chem 25:1521

9. Geuenich D, Hess K, Köhler F, Herges R (2005) Anisotropy of the induced current density (ACID), a general method to quantify and visualize electronic delocalization. Chem Rev 105:3758

10. Hirshfeld FL (1977) Bonded-atom fragments for describing molecular charge densities. Theor Chem Acc 44:129

11. Lu T, Chen F (2012) Atomic dipole moment corrected Hirshfeld population method. J Theor Comput Chem 11:163

12. Lu T, Chen F (2012) Comparison of computational methods for atomic charges. Acta Phys Chim Sin 28:1

13. Lu T, Chen F (2013) Bond order analysis based on the Laplacian of electron density in fuzzy overlap space. J Phys Chem A 117:3100

14. Bader FW (1994) Atoms in molecules: a quantum theory. Oxford University Press, New York

15. Rong C, Lu T, Liu S (2014) Dissecting molecular descriptors into atomic contributions in density functional reactivity theory. J Chem Phys 140:024109

16. Mulliken RS (1955) Electronic population analysis on LCAO-MO molecular wave functions. II. Overlap populations, bond orders, and covalent bond energies. J Chem Phys 23:1841

17. Becke AD, Edgecombe KE (1990) A simple measure of electron localization in atomic and molecular systems. J Chem Phys 92:5397

18. Fuentealba P, Chamorro E, Santos JC (2007) Understanding and using the electron localization function. In: Toro-Labbé A (ed) Theoretical aspects of chemical reactivity. Elsevier, Amsterdam, p 57

19. Lu T, Chen F (2011) Meaning and functional form of the electron localization function. Acta Phys Chim Sin 27:2786

20. Lu T, Chen Q (2018) Revealing molecular electronic structure via analysis of valence electron density. Acta Phys Chim Sin 34:503

21. Manzetti S, Lu T (2013) Alternant conjugated oligomers with tunable and narrow HOMO-LUMO gaps as sustainable nanowires. RSC Adv 3:25881

22. Manzetti S, Lu T, Behzadi H, Estrafili MD, Thi Le H-L, Vach H (2015) Intriguing properties of unusual silicon nanocrystals. RSC Adv 5:78192

23. Savin A, Jepsen O, Flad J, Andersen OK, Preuss H, von Schnering HG (1992) Electron localization in solid-state structures of the elements: the diamond structure. Angew Chem Int Ed Engl 31:187

24. Santos JC, Andres J, Aizman A, Fuentealba P (2004) An aromaticity scale based on the topological analysis of the electron localization function including σ and π contributions. J Chem Theory Comput 1:83

25. Santos JC, Tiznado W, Contreras R, Fuentealba P (2004) Sigma-Pi separation of the electron localization function and aromaticity. J Chem Phys 120:1670

26. Liu S, Rong C, Lu T, Hu H (2018) Identifying strong covalent interactions with pauli energy. J Phys Chem A 122:3087

27. Astakhov AA, Tsirelson VG (2014) Spatial localization of electron pairs in molecules using the fisher information density. Chem Phys 435:49

28. Schmider HL, Becke AD (2000) Chemical content of the kinetic energy density. J Mol Struct (THEOCHEM) 527:51

29. Tsirelson V, Stash A (2002) Analyzing experimental electron density with the localized-orbital locator. Acta Crystallogr Sect B Struct Sci 58:780

30. Jacobsen H (2013) Bond descriptors based on kinetic energy densities reveal regions of slow electrons—another look at aromaticity. Chem Phys Lett 582:144

31. Giambiagi M, de Giambiagi M, Mundim K (1990) Definition of a multicenter bond index. Struct Chem 1:423

32. Kar T, Sánchez Marcos E (1992) Three-center four-electron bonds and their indices. Chem Phys Lett 192:14

33. Ponec R, Mayer I (1997) Investigation of some properties of multicenter bond indices. J Phys Chem A 101:1738

34. Yu D, Rong C, Lu T, De Proft F, Liu S (2018) Baird's rule in substituted fulvene derivatives: an information-theoretic study on triplet-state aromaticity and antiaromaticity. ACS Omega 3:18370

35. Matito E (2016) An electronic aromaticity index for large rings. Phys Chem Chem Phys 18:11839

36. Mayer I (1983) Charge, bond order and valence in the AB initio SCF theory. Chem Phys Lett 97:270

37. Matito E, Poater J, Solà M, Duran M, Salvador P (2005) Comparison of the AIM delocalization index and the mayer and fuzzy atom bond orders. J Phys Chem A 109:9904

38. Lu T, Chen F (2012) Multiwfn: a multifunctional wavefunction analyzer. J Comput Chem 33:580

39. Lu T, Chen F (2011) Calculation of molecular orbital composition. Acta Chim Sin 69:2393

40. Ros P, Schuit GCA (1966) Molecular orbital calculations on copper chloride complexes. Theor Chem Acc 4:1

41. Szabo A, Ostlund NS (1989) Modern quantum chemistry. Dover Publications, New York

42. Pipek J, Mezey PG (1989) A fast intrinsic localization procedure applicable for ab initio and semiempirical linear combination of atomic orbital wave functions. J Chem Phys 90:4916

43. Edmiston C, Ruedenberg K (1963) Localized atomic and molecular orbitals. Rev Mod Phys 35:457

44. Reed AE, Schleyer PVR (1990) Chemical bonding in hypervalent molecules the dominance of ionic bonding and negative hyperconjugation over d-orbital participation. J Am Chem Soc 112:1434

45. Jensen F (2007) Introduction to computational chemistry. Wiley, West Sussex

46. Foster JM, Boys SF (1960) Canonical configurational interaction procedure. Rev Mod Phys 32:300

47. Martin RL (2003) Natural transition orbitals. J Chem Phys 118:4775

48. Weinhold F (1998) Natural bond orbital methods. In: Schleyer PVR (ed) Encyclopedia of computational chemistry, vol 2. Wiley, West Sussex, p 1792

49. Frisch MJ, Trucks GW, Schlegel HB, Scuseria GE, Robb MA, Cheeseman JR, Scalmani G, Barone V, Petersson GA, Nakatsuji H, Li X, Caricato M, Marenich AV, Bloino J, Janesko BG, Gomperts R, Mennucci B, Hratchian HP, Ortiz JV, Izmaylov AF, Sonnenberg JL, Ding WF, Lipparini F, Egidi F, Goings J, Peng B, Petrone A, Henderson T, Ranasinghe D, Zakrzewski VG, Gao J, Rega N, Zheng G, Liang W, Hada M, Ehara M, Toyota K, Fukuda R, Hasegawa J, Ishida M, Nakajima T, Honda Y, Kitao O, Nakai H, Vreven T, Throssell K, Montgomery JA Jr, Peralta JE, Ogliaro F, Bearpark MJ, Heyd JJ, Brothers EN, Kudin KN, Staroverov VN, Keith TA, Kobayashi R, Normand J, Raghavachari K, Rendell AP, Burant JC, Iyengar SS, Tomasi J, Cossi M, Millam JM, Klene M, Adamo C, Cammi R, Ochterski JW, Martin RL, Morokuma K, Farkas O, Foresman JB, Fox DJ (2016) Gaussian 16. Wallingford, CT

50. Hariharan PC, Pople JA (1973) The influence of polarization functions on molecular orbital hydrogenation energies. Theor Chem Acc 28:213

51. Stephens PJ, Devlin FJ, Chabalowski CF, Frisch MJ (1994) Ab initio calculation of vibrational absorption and circular dichroism spectra using density functional force fields. J Phys Chem 98:11623

52. Humphrey W, Dalke A, Schulten K (1996) VMD: visual molecular dynamics. J Mol Graph 14:33

53. Deng Y, Yu D, Cao X, Liu L, Rong C, Lu T, Liu S (2018) Structure, aromaticity and reactivity of corannulene and its analogues: a conceptual density functional theory and density functional reactivity theory study. Mol Phys 116:956

54. Perdew JP (1986) Density-functional approximation for the correlation energy of the inhomogeneous electron gas. Phys Rev B 33:8822

55. Becke AD (1988) Density-functional exchange-energy approximation with correct asymptotic behavior. Phys Rev A 38:3098

56. Andrae D, Häußermann U, Dolg M, Stoll H, Preuß H (1990) Energy-adjustedab initio pseudopotentials for the second and third row transition elements. Theor Chim Acta 77:123

57. Sedlak R, Janowski T, Pitoňák M, Řezáč J, Pulay P, Hobza P (2013) Accuracy of quantum chemical methods for large noncovalent complexes. J Chem Theory Comput 9:3364

58. Johnson ER, Keinan S, Mori-Sánchez P, Contreras-García J, Cohen AJ, Yang W (2010) Revealing noncovalent interactions. J Am Chem Soc 132:6498

59. For manual corresponding to Multiwfn Version 3.7, see section 4.100.22 on how to perform analyses similar to this work. The steps of realizing topology analysis of ELF-π is illustrated in section 4.5.3. The way of rendering isosurface maps by VMD program based on the data calculated by Multiwfn is introduced in section 4.A.14. The manual is freely available at http://sobereva.com/multiwfn Accessed on 30 Sep 2019